

**Specific Primary Ionization
Induced by Minimum Ionizing Electrons
in CH₄, C₂H₆, C₃H₈, i-C₄H₁₀, Ar, DME, TEA and
TMAE**

G. Malamudⁱ, A. Breskin, R. Chechikⁱⁱ and A. Pansky

Nuclear Physics Department
The Weizmann Inst. of Science
76100, Rehovot, ISRAEL

ABSTRACT

Specific Primary Ionization induced by minimum ionizing electrons has been measured in several gases and vapors. Charges deposited by β -electrons in a low pressure gas, were collected, amplified by a multistep gaseous electron multiplier and counted. The high counting efficiency of the multiplier provided results of systematically higher values as compared to existing data. The respective values of the specific primary ionization in CH₄, C₂H₆, C₃H₈, i-C₄H₁₀, Argon, DME (Dimethylether), TEA (Triethylamine) and TMAE [Tetrakis(dimethylamino)ethylene] are: 0.034, 0.065, 0.095, 0.12, 0.03, 0.082, 0.0195 and 0.370 *clusters/cm·Torr*. We present the experimental method and discuss the results and their accuracy.

ⁱCurrent address: LPNHE-Ecole Polytechnique, Palaiseau, France

ⁱⁱThe Hettie H. Heineman Research Fellow

1 Introduction

The physical mechanism of primary ionization is, in principle, simple and well understood [1, 2]. However, an exact theoretical calculation of the absolute specific primary ionization (SPI) values is rather complicated for most atoms and molecules. Models which take into account the full photoabsorption cross section for ionization, σ_{γ} , were developed [3, 4]. In some cases, where the calculations were too complicated, experimental data of σ_{γ} were obtained with the advent of synchrotron radiation sources. Yet, approximated computer simulation programs were needed for the final extraction of the SPI.

A good knowledge of the SPI, induced by relativistic charged particles in matter, is of practical importance in many fields, in particular for the design of radiation detectors for particle identification [5]. Only few attempts have been made to measure the SPI in gases. The first attempts consisted of a direct-counting of primary ionization clusters along particle tracks in cloud-chambers [6 - 11]. However, the density of primary clusters was too high to allow an efficient separation and counting. Another method which was employed was the extraction of the value of SPI via the determination of the inefficiency of a gas-filled counter, referred in this paper as the 0-counting method. The method was first used by Graf [12] in measurements in air, and later by McClure, who measured the SPI in H_2 , He, Ne and Ar [13]. An improved experiment was then carried out by Rieke et.al. who measured the SPI of relativistic electrons in a large variety of gases. In their work the induced ionization was detected through electron amplification, in proportional or Geiger-Müller multiplication modes. A comprehensive summary of their work can be found in ref. [14]. SPI values in DME and Ar were measured recently also by Bouclier et.al. [15] in a cylindrical multidrift tube and with cosmic rays. Their SPI values obtained by the 0-counting method are, however, of an inferior accuracy as compared to those of Rieke et.al.

A charged particle traversing a medium may undergo energy transfers along its track. The energy is transferred through collisions with atomic electrons. In each collision with an energy transfer greater than the binding energy E_j of the target electron, a primary

electron may be ejected. In collisions with energy transfers smaller than E_j , an excitation of the atom (or molecule) occurs. The excitation energy may be released in many ways, like collisional thermalization or photon emission, usually not leading to further ionization. However, in some cases ionization may occur via the Penning effect in gas mixtures, or via associative ionization [14]. In all these ionizing processes at least one primary electron is ejected, and they are all referred to here as primary ionizing collisions. The statistical behaviour of the number of primary collisions, induced by monoenergetic charged particles along a constant track length is Poisson-like. The primary electrons may release secondary electrons, depending on their initial kinetic energy, so that in each collision a primary cluster of size $N_e \geq 1$ is generated. Most of the primary clusters ($\approx 65 - 80\%$, [3, 16]) are single electrons. Therefore, a mandatory requirement for any counting or detection method, is a very high efficiency for single electron detection.

In the present article we report on the measurement of SPI in some gases and vapors: CH_4 , C_2H_6 , C_3H_8 , $i\text{-C}_4\text{H}_{10}$, Argon, DME, TEA and TMAE. Two counting methods were used: a direct-counting of the primary electron clusters, and the 0-counting method are described in sect.2. A detailed error evaluation is given in sect.3. The results were cross-checked with computer simulations, taking into account several physical parameters like electron diffusion and drift velocity in the conversion volume, ionization density and cluster size distribution, detector gain and single electron amplification statistics, pulse shape etc. The ionization electrons were detected in a proportional amplification mode, in a low-pressure multistep electron multiplier [17]. The high gain ($>10^7$) ensured a detection efficiency close to 100% for single electrons.

A detailed discussion of the cluster counting method and its application to particle identification is given in refs. [18 - 20]. Therefore, experimental details and procedures will be discussed only briefly.

2 The experimental technique

2.1 SPI counting methods

Two SPI-counting methods have been employed:

Direct-counting: The primary electron clusters along individual particle tracks are identified and counted. The expected average primary ionization, $\langle N_p \rangle$, is given by

$$\langle N_p \rangle = 1/N \cdot \sum_i^N N_{pi} \quad (1)$$

where N is the number of measured tracks and N_{pi} is the number of counted primary clusters in a given track i . The intrinsic statistical error of the measured mean $\langle N_p \rangle$ is determined by the Poisson nature of the process:

$$\sigma(\langle N_p \rangle) = \sqrt{\langle N_p \rangle / (N - 1)} \quad (2)$$

In the case of a direct-counting of the number of primary collisions, a necessary condition which indicates that the counting procedure is correct, is the observation of a Poissonian distribution of the N_{pi} 's, with a standard deviation $\sigma(N_p) = \sqrt{\langle N_p \rangle}$.

It should be noted that this method is sensitive to effects caused by multiple-electron cluster ($N_e \geq 2$) dissociation and by other detection imperfections, like cluster mixing, single electron losses or parasitic secondary avalanches. The contributions of these effects to the systematic experimental errors are discussed in sect.3 and in more detail in refs. [18] and [19].

0-counting: Given an average number of primary collisions (N_p) along the particle track, the probability $P_{N_p=0}$ for no ionizing collision to occur in an individual event ($N_p = 0$) is given by:

$$P_{N_p=0} = e^{-\langle N_p \rangle} \quad (3)$$

Therefore in a set of N measurements, of which in N_0 events no collisions occurred (0-counts), and assuming full electron detection efficiency, the expected value of the average

primary ionization is:

$$\langle N_p \rangle = -\ln(N_0/N) \quad (4)$$

The intrinsic statistical error is given by

$$\sigma(\langle N_p \rangle) = \frac{N - N_0}{N \cdot N_0} \quad (5)$$

It should be noted that as the events are separated into only two types, events in which any number of clusters was counted and events in which no cluster was counted, the measured $\langle N_p \rangle$ is not affected either by cluster overlapping or dissociation or by secondary parasitic avalanches. The systematic errors related to the 0-counting method are discussed in sect.3 and refs. [18 - 20].

The SPI values presented in this work are expressed in a normalized unit of *clusters/cm·Torr*, and are given for room temperature conditions ($T=294^\circ K$). The SPI value at other temperature T is derived from : $SPI_T = SPI_{294} \cdot [\rho_T/\rho_{294}]$, ρ being the gas density.

2.2 Primary ionization detection

The primary ionization detector is shown in fig.1. It consists of a radiation conversion volume followed by a high gain two-stage electron multiplier [21, 22]. The detector operates at low gas pressure, typically 2-20 Torr.

Particles enter the conversion volume in parallel to the electric field direction. A trail of primary clusters is formed along the particle track. The clusters, of single or several electrons, drift towards the amplification region. In order to have good separation between primary clusters, which is important in the case of direct-counting, the reduced electric field (E/p) in the conversion region must be kept low, in order to reach low drift velocities. The arrival of individual clusters to the amplification region is thus *time-expanded* [23]. The drift velocity in the conversion region is adjusted to minimize the dissociation of the N_p primary clusters by diffusion, while still enabling an efficient separation between them. Avalanches induced by individual electron clusters along the pulse-trail are further amplified by electronic means and analyzed.

The main advantages of measuring the SPI with this technique are:

- The average single-electron amplification factor reaches values of up to 10^8 per avalanche, before sparking probability is significant. Therefore, the detection efficiency for single electrons is very close to 100%.
- Low ionization density in the low pressure gas. In the case of direct-counting this allows for a good separation between primary clusters. It also avoids operation at very low drift velocities in the conversion volume, which might result in electron losses by recombination and in electron cluster dissociation by diffusion. In the case of 0-counting, the higher number of 0-events at lower $\langle N_p \rangle$ values (eq.3) reduces the number of measured tracks necessary for a high statistical accuracy (eq.5).

The analog primary-cluster pulse trails are digitized and stored in a computer for off-line analysis. Each digitized cluster-track is correlated [24] to a search spectrum, $S(t)$, representing a typical single electron avalanche pulse shape. To find the primary cluster peaks, a correlation spectrum, $C(\tau)$, is calculated:

$$C(\tau) = \sum_{t=1}^{N_T} S(t) \cdot [Y(\tau + t) - A_\tau] \quad (6)$$

where N_T is the number of sampling points of the search spectrum and A_τ is the average of the data spectrum, $Y(i)$, calculated over the summation points:

$$A_\tau = \left(\frac{1}{N_T} \right) \cdot \sum_{i=\tau}^{\tau+N_T-1} Y(i) \quad (7)$$

Peaks above an appropriate threshold in the correlated spectrum $C(\tau)$ are detected in a differential manner and counted by the analysis software. Fig.2 shows a track produced by minimum ionizing β^- particle in DME, and the corresponding correlated spectrum. Peaks which are recognized by the correlation technique are circled. The high cluster separation and detection efficiencies are well apparent.

While measurements in hydrocarbons and many molecular gases are rather simple, in noble gases it is impossible to reach a high proportional gain, due to poor photon quenching. In such cases, where the specific ionization in a gas of interest (denote: SPI(A)) cannot be measured, a measurement in a mixture of this gas with another gas (denote:

B), with a known $SPI(B)$, may provide the value of $SPI(A)$, assuming a linear dependence of the primary ionization on the relative molecular concentrations (this assumption is valid for cases in which the Penning-effect contribution to the ionization is negligible (see sect.1)):

$$SPI(A) = \frac{SPI_t - C_B \cdot SPI(B)}{C_A} \quad (8)$$

where SPI_t is the specific ionization of the gas mixture, C_A and C_B are the relative molecular concentrations of gases A and B correspondingly.

More details about the operation of the detector, the readout system and track analysis can be found in refs. [18 – 20].

2.3 Experimental set-up

The detector (fig.1) consists of a stack of circular mesh electrodes, mounted on epoxy resin frames. The electrodes, of an active area of 50 cm^2 , are made of stainless-steel mesh, with $50 \mu\text{m}$ wire diameter and a pitch of $500 \mu\text{m}$. The conversion volume length was adjusted according to the counting method: 14-20 cm in the case of the direct-counting method, and 3.3-3.6 cm for the 0-counting method. The uniformity of the electric field within the long conversion volume is assured by equally spaced copper strips, printed on the inner face of a cylinder made of a thin insulating foil. The electrodes in each parallel grid amplification element are 3.2 mm apart. The entrance and exit radiation windows are made of $25 \mu\text{m}$ thick Mylar film. A collimated $^{106}\text{Ru} \beta^-$ source ($E_{\text{max}}=3.54 \text{ MeV}$) was used. Electrons with an energy in the minimum ionization regime were selected using two scintillators in coincidence, placed in front of and behind the detector. A 2.5 mm thick G-10 absorber, mounted in front of the second scintillator, ensured that only electrons with energies $E > 1 \text{ MeV}$ could generate a trigger signal. The opening angle defined by the electron collimator and the two scintillators is $\pm 5^\circ$. The coincidence signal of the two scintillators triggered the digitizing oscilloscope for data readout.

The detector was operated in a differential flow mode in a pressure range of 2-12 Torr. The pressure inside the detector was measured with an MKS Baratron, with an accuracy better than 0.05 Torr. The purity of gases was: CH_4 and C_2H_6 : 99.95% C_3H_8

and i -C₄H₁₀: 99.5%, Ar: 99.999% and DME: 99.9%. Vapor pressures of liquid TEA and TMAE were controlled by heating the liquid vessel to temperatures providing vapors at pressures higher than the detector operating pressure. The purity of TEA was higher than 99% (Merck, art. 808352) and that of TMAE much superior (vacuum distilled by Bayer, Germany). The detector pressure was adjusted, as for the gases, by differential pumping. In this case the detector was kept at higher temperatures, so as to avoid condensation.

Electric pulses induced by the electron avalanches on the anode of the second amplification stage were amplified by a low-noise current amplifier. The amplified electron pulse trails were recorded by a PC-controlled fast digitizing oscilloscope (Tektronix RTD-710, 200 MHz sampling rate). The data was stored in the computer memory and analyzed off-line.

3 Error evaluation

The *intrinsic* statistical errors related to the two counting methods are formulated by eqns.2 and 5. In this section we discuss the possible systematic errors related to the measuring conditions or to calibration procedures.

Sources of systematic errors common to both counting methods are:

Variation in the incoming electron energy: Electrons are at minimum ionization at $\beta\gamma \approx 3.3 - 3.4$, depending on the specific gas under consideration. Electrons which are slightly off minimum ionization would produce a higher average ionization. Our calculations, based on Bethe's formulation as used in Ref. [14], which take into account the selected energy range of 1-3.54 MeV, show that the total expected over-ionization is below 1%.

Pressure and temperature uncertainty: The effects of some inaccuracy in the measurement of the pressure and the temperature in the detector, on the measured SPI, are estimated to be smaller than 1%.

Systematic errors related to the direct-counting method are:

Primary cluster overlapping and dissociation: Two cluster-pulses which are too

close to each other may overlap. This may lead to a loss of electrons, and therefore to an underestimation of the true SPI value. On the other hand clusters of size $N_e > 1$ are dissociated by diffusion in the course of their drift towards the amplification region, leading to an overcounting of primary clusters. The importance of these phenomena depends on the ionization density, width of single electron pulses, electron drift velocity in the conversion region, the longitudinal diffusion in the gas under consideration and the analysis parameters. In a previous study of these effects on the primary cluster counting accuracy [18, 19] we found that they are the main error source while using direct-counting. In all our measurements the working conditions were set so that Poisson distributions were observed for pulses recorded from a short section, in the middle of the conversion volume [18]. At the low gas pressures used in these experiments (2-12 Torr) the variations of the measured SPI values under various experimental conditions were of the order of 5-10%. These results were confirmed by Monte-Carlo simulations (see sect.4).

Other error sources: Electrons may be lost due to insufficient amplification or due to attachment or recombination in the course of their drift process, which will lead to an undercounting of primary clusters. On the other hand the production of secondary parasitic avalanches will cause an overcounting of the primary clusters. The effect of these phenomena was estimated to be negligible as compared to the effects of cluster overlapping and dissociation [18, 19]. We should also note a possible error in the determination of the active conversion volume length, mostly due to electric field penetration from the amplification gap. We estimated the maximal error due to this effect to be of the order of the half mesh wire spacing, namely ± 0.25 mm.

In our experiments the statistical errors were much smaller than the systematic errors, and the overall experimental error of the direct-counting method was estimated to be $\pm 10\%$.

Systematic errors related to the 0-counting method are:

Inefficiency for single electron detection: The effect of the loss of electrons due to insufficient detector amplification, which leads to an underestimation of the SPI values, was carefully studied by us, as we believe that this is the main reason for the lower results

measured by other authors [13, 14] (see sect 5).

This effect was estimated by the following procedure:

1. For a given average number of primary collisions $\langle N_p \rangle$ per track, we calculate the probability P_{N_p} for N_p primary clusters to be induced. P_{N_p} is given by Poisson statistics:

$$P_{N_p} = \frac{\langle N_p \rangle^{N_p} \cdot e^{-N_p}}{N_p!} \quad (9)$$

2. We calculate the probability P_{N_e} for N_e electrons to be induced. P_{N_e} is obtained as follows:

$$\begin{aligned} P_{N_e=0} &= P_{N_p=0} \\ P_{N_e=1} &= P_{N_p=1} \cdot P(\text{CS} = 1) \\ P_{N_e=2} &= P_{N_p=2} \cdot P^2(\text{CS} = 1) + P_{N_p=1} \cdot P(\text{CS} = 2) \\ P_{N_e=3} &= P_{N_p=3} \cdot P^3(\text{CS} = 1) + 2 \cdot P_{N_p=2} \cdot P(\text{CS} = 1) \cdot P(\text{CS} = 2) + \\ &\quad P_{N_p=1} \cdot P(\text{CS} = 3) \end{aligned} \quad (10)$$

etc...

where $P(\text{CS} = n_e)$ is the probability for a primary electron cluster to contain n_e electrons [3, 16].

3. We calculate the probability $P_{N_p=0}(\text{observed})$ to observe 0-clusters in a given event. $P_{N_p=0}(\text{observed})$ is given by:

$$P_{N_p=0}(\text{observed}) = P_{N_e=0} + P_{N_e=1} \cdot (1 - \epsilon) + P_{N_e=2} \cdot (1 - \epsilon)^2 + \dots \quad (11)$$

where ϵ is the detector efficiency for single electron detection.

Table 1 shows the resulting undercounting due to single electron losses in a realistic example of measuring the specific primary ionization in Ethane (SPI=0.065 clusters/cm·Torr, p: 7 Torr; conversion gap: 3.32 cm). For the cluster size distribution we used data calculated by Lapique & Piuz [3].

For all our measurements we verified that N_p is not sensitive to small changes in the detector gain. We estimated that the single electron detection efficiency of our counting method was higher than 98%. It is shown that in this case our undercounting error should

be smaller than 1.7%.

Determination of the conversion length: Due to the shorter conversion length used for the 0-counting, the effect of inaccuracy in its determination is larger compared to the direct-counting method. An aluminized mylar foil was used as the endcap electrode of the conversion volume (no field leakage) in order to minimize this inaccuracy. We estimated the error due to this effect to be ± 0.25 mm ($\approx 0.8\%$).

Ejection of secondary electrons from the endcap electrode: The probability of ejecting a secondary electron from the aluminized mylar foil is below 1% . In a typical case where $P_{N_p=0} = 0.1$ the error in $\langle N_p \rangle$ is $\approx 0.5\%$.

The overall systematic errors were estimated to be of the order $-2+4\%$, and were added to the statistical errors to determine the total experimental error (Table 2).

4 Results

Our measured SPI values are summarized in table 2. Corresponding results (when existing) measured by Rieke et.al. [14] are presented for comparison. The differences are discussed in sect.5. We discuss below, in some detail, a part of our experimental results with some of the examined gases, which clarify (and support) the steps and considerations which led to the final presentation of table 2.

Isobutane:

Direct-counting: Different measurements were made as a function of the drift velocity in the conversion volume. SPI values of 0.129, 0.126, 0.114 and 0.109 *clusters/cm.Torr* were measured for respective drift velocities of 1.71, 1.89, 2.46 and 2.79 $\text{cm}/\mu\text{s}$ ($p=10$ Torr; conversion length: 20.4 cm; statistical error is smaller than 1%). The increase in the measured SPI at lower drift velocities is due to the combined effects of higher primary cluster dissociation and the higher pulse resolution due to the time-expansion of the arrival of primary clusters to the amplification region. The variations are of the order of 5-10%. Similar results were obtained with other conversion lengths and at different pressures. In order to verify our working conditions we introduced the measured SPI value of 0.12 *clusters/cm.Torr* into a Monte-Carlo simulation program, which simulates the creation,

transport, amplification and counting of the primary clusters in the detector volume (see Refs.[18, 19]). The resulting SPI values were all within $\pm 5-10\%$ deviation from the input value. The only way to impair this agreement was to use unrealistic input parameters, like a very large diffusion, very narrow pulse width or a cluster size distribution which is very different from those presented in refs.[3, 16]. We concluded that the error on the measured SPI values is $\leq 10\%$.

0-counting: Table 3 summarizes the measured values of the SPI under various experimental conditions. The deviations of the different values from the average ($0.12 \text{ clusters/cm}\cdot\text{Torr}$) are within the expected statistical errors. The overall statistical inaccuracy of the measured SPI is $< 1.5\%$.

Propane:

Direct-counting: Measurements were done at three different gas pressures: 8, 10 and 12 Torr. The results are summarized in table 4. The average measured SPI in Propane is $0.097 \text{ clusters/cm}\cdot\text{Torr}$. Notice that over the whole pressure range the variations in the measured ionization densities are smaller than $\pm 1\%$. However, it should be emphasized that, as in the case of Isobutane, variations of the order of $\pm 5 - 10\%$ were measured at other drift velocities, which provided N_p distributions which are narrower or broader than Poisson. Therefore, we estimate our measurement accuracy to be of that order.

0-counting: The value of the specific primary ionization is $0.095 \text{ clusters/cm}\cdot\text{Torr}$, with a statistical error of $\pm 1.5\%$.

Methane:

Direct-counting: We measured an SPI value of $0.047 \text{ clusters/cm}\cdot\text{Torr}$. The experimental conditions were: $p=10 \text{ Torr}$; $w=6.53 \text{ cm}/\mu\text{s}$; conversion length: 20.4 cm . However, the measurements encountered a serious problem of secondary photon emission, leading to parasitic avalanches, which results in an overestimation of the SPI. Therefore we could not estimate the accuracy of the measurement.

0-counting: The value of the specific primary ionization is $0.034 \text{ clusters/cm}\cdot\text{Torr}$, with a statistical accuracy of $\pm 1.5\%$. Notice the considerable difference between this result and that measured by direct-counting, due to the insensitivity of the 0-counting method

to secondary avalanches.

Triethylamine (TEA):

Direct-counting: The specific primary ionization was measured at a vapor pressure of 5.2 Torr. The drift velocity in the conversion volume was 2.24 cm/ μ s. The The specific primary ionization value was found to be 0.19 ($\pm 10\%$) *clusters/cm·Torr*.

0-counting: The SPI value is 0.195 *clusters/cm·Torr*, with a statistical error of $\pm 2.5\%$.

Tetrakis(dimethylamino)ethylene (TMAE):

The specific primary ionization in TMAE was measured only by the 0-counting method. The detector was operated with pure TMAE vapor at pressures of 1.48-2.32 Torr. The results are summarized in table 5. We concluded that the specific primary ionization in TMAE is 0.37 *clusters/cm·Torr*, with a statistical error of about $\pm 1.5\%$.

Argon:

The specific primary ionization of Argon was measured, using gas-mixtures of Ar/*i*-C₄H₁₀ and Ar/C₂H₆, at various pressures and concentrations. The SPI was extracted by a simple linear fit (see eq.8) of data measured at many different gas concentrations.

Direct-counting: The variations of the calculated values of the SPI under different conditions were large: between 0.025 and 0.047 *clusters/cm·Torr*. The reason, which follows from Eq.8, is that SPI(*A*) is the result of the difference between two measured values. Therefore, the lower the value of SPI(*A*), the higher is the resulting relative error.

0-counting: Keeping in mind that here most of the possible systematic measurement errors, are independent of the electron drift velocity (cluster dissociation) and not sensitive to secondary parasitic avalanches, it is expected that systematic errors will have the same effect for all measurements. We used Ar/C₂H₆ mixtures with relative Ar concentrations which varied between 0 to 28%. The estimated specific ionization of Argon is 0.029 *clusters/cm·Torr*, with a statistical error of $\pm 10\%$. The relatively large statistical error, as compared to measurements with pure gases, arises from the low Argon concentrations required for a high detector gain.

5 Summary and discussion

The specific primary ionization (SPI) induced by minimum ionizing electrons was measured in several gases and vapours: CH_4 , C_3H_8 , C_2H_6 , $i\text{-C}_4\text{H}_{10}$, Argon, Dimethyl-Ether (DME), Triethylamine (TEA) and Tetrakis (dimethylamino)ethylene (TMAE). The SPI in the last two vapors is given here for the first time.

A novel method was applied, based on the ionization in a low-pressure gas volume, followed by the transport, multiplication and counting of ionization electron clusters, with a highly efficient multistage electron multiplier. The clusters were recognized by a computerized correlation technique.

Two methods were applied, a direct-counting of the ionization clusters along particle tracks and a 0-counting method, namely the measurement of the relative number of events where no ionization occurred in a given gas volume.

The low ionization density at low gas pressures allows for a good separation between primary clusters in the case of a direct-counting (except for CH_4), and a better statistical accuracy with the 0-counting technique. The statistical and systematic errors related to the two SPI measuring techniques have been discussed in detail in the text. It appears that the direct-counting method, though reflecting directly the physical primary ionization process, has various drawbacks in the present application. They are mostly related to electron losses due to cluster mixing and to overcounting due to cluster dissociation during the transport process in the conversion volume and due to secondary parasitic avalanches. This is reflected in the rather large fluctuations, of the order of $\pm 10\%$, in the SPI measurements.

As can be seen in table 2, summarizing our results, the values of the specific primary ionization measured by us are systematically higher than those measured by Rieke et.al. [14] (which are generally in very good agreement with the results obtained by McClure [13]). In the case of Argon our value is lower, but one should notice our relatively large statistical error. The experimental errors quoted by Rieke et.al. (0.5-1.5%) are smaller than the differences between the two data sets. This may be explained by an over-

estimation, by Rieke et.al., of their efficiency for single electron detection. We note also that these authors used, for all gases under consideration except Argon, a proportional mode of amplification, and that they were not able to accurately estimate their relative electron loss due to insufficient amplification. Our calculated experimental errors due to electron losses are very low, as shown in table 1. We therefore conclude that our higher SPI values are probably due to the very high efficiency of our technique for detecting single electrons.

The quality of our results in noble gases, like Argon, mixed with hydrocarbons of a known SPI value, is inferior to that of pure gases or vapors. We believe that an improvement in our experimental accuracy will, in the future, allow the measurement of noble gases with better reliability.

We would like to thank H.Aclander for helpful discussions. We are also grateful to M.Klin and Y.Gil for their technical support.

References

- [1] H. A. Bethe. *H. B. der Phys.*, Vol. 24.1 p.518, edit. by Geiger and Sheel, publisher: Julius Springer Verlag, Berlin, 1933.
- [2] H. A. Bethe and J. Ashkin. In E. Segre, editor, *Experimental Nucl. Physics*, volume 1. John Wiley & Sons, New York, 1953.
- [3] F. Lapique and F. Piuz. *Nucl. Inst. & Methods*, 175:315–323, 1980.
- [4] W.W. Allison and J.H. Cobb. *Ann. Rev. Nucl. Part. Sci.*, 30:253–298, 1980.
- [5] J. Va'vra. *Nucl. Inst. & Methods*, A224:391–415, 1986.
- [6] C.T.R. Wilson. *Proc. of Royal Society (London)*, A104:192, 1923.
- [7] E.J. Williams and F.R. Terroux. *Proc. of Royal Society (London)*, A126:289, 1930.
- [8] J.T. Tate and P. T. Smith. *Phys. Rev.*, 39:272, 1932.
- [9] W.E. Danforth and W.E. Ramsey. *Phys. Rev.*, 49:854, 1936.
- [10] M.G.E. Cosyns. *Nature*, 139:802, 1937.
- [11] F.L. Hereford. *Phys. Rev.*, 74:574, 1948.
- [12] T. Graf. *J. Phys. Radium*, 10:513, 1939.
- [13] G.W. McClure. *Phys. Rev.*, 90-3:796–803, 1953.
- [14] F.F. Rieke. and P. William. *Phys. Rev. A*, 6-4:1507–1519, 1972.
- [15] R. Bouclier, J. Gaudaen, I. Gouz, B. Guerard, J.C. Santiard, F. Sauli, and R. Wojcik. *Nucl. Inst. & Methods*, A283:509–514, 1989.
- [16] H. Fischle, J. Heintze, and B. Schmidt. *Nucl. Inst. & Methods*, A301:202–214, 1991.
- [17] A. Breskin, G. Charpak, and S. Majewski. *Nucl. Inst. & Methods*, 220:349, 1984.

- [18] G. Malamud, A. Breskin, and R. Chechik. *Nucl. Inst. & Methods*, A307:83-96, 1991.
- [19] G. Malamud. The Study of a Novel Method for Measuring Specific Radiation Induced Ionization in Gases. PhD thesis, Weizmann Inst. of Science, Rehovot, Israel, 1992.
- [20] A. Pansky, G. Malamud, A. Breskin, and R. Chechik. "Applications of Gaseous Electron Counting Detectors", Presented at the Vienna Conf. on Wire chambers, Vienna, February 1992. To be published in *Nucl. Inst. & Methods*.
- [21] A. Breskin, G. Charpak, S. Majewski, G. Melchart, and F. Sauli. *Nucl. Inst. & Methods*, 161:19, 1979.
- [22] A. Breskin and R. Chechik. *Nucl. Inst. & Methods*, A252:488-497, 1986, and references therein.
- [23] H.A. Walenta. *IEEE Trans. on Nucl. Sci.*, NS-26:73-80, 1979.
- [24] W.W. Black. *Nucl. Inst. & Methods*, 71:317-327, 1969.

Figure Captions

1. A schematic view of the low pressure cluster counting detector.
2. Example of a measured (a) and a correlated (b) minimum ionizing β^- electron cluster track. $p=10$ Torr DME; drift velocity: $3.4 \text{ cm}/\mu\text{s}$, conversion length: 20.4 cm. Total track length : $6 \mu\text{s}$. Electron pulses recognized by the correlation technique are circled. The horizontal line in (b) indicates the threshold used in the analysis.

Table Captions

1. Calculated errors in the specific primary ionization measured by the 0-counting method, due to inefficiency for single electron detection. Conditions: 7 Torr of C_2H_6 ; conversion length: 3.32 cm.
2. Summary of the measured values of the specific primary ionization, induced by minimum ionizing β -electrons in gases. The given accuracies take into account statistical and systematic errors. Results of measurements by Rieke et.al [14] are presented as well, their overall quoted error is $\leq 1.4\%$. All the results are normalized to a temperature of $21^\circ C$.
3. Specific primary ionization (SPI) induced by minimum ionizing electrons in $i-C_4H_{10}$, measured at various experimental conditions, by the 0-counting method. Conversion gap: 3.32 cm. Results are normalized to a temperature of $21^\circ C$.
4. Specific primary ionization (SPI) induced by minimum ionizing electrons, directly counted in C_3H_8 at various gas pressures. Conversion length: 20.4 cm; Statistical accuracy: better than 1%. Results are normalized to a temperature of $21^\circ C$.
5. Specific primary ionization (SPI) induced by minimum ionizing electrons in TMAE, measured at various experimental conditions using the 0-counting method. Conversion gap: 3.32 cm. Results are normalized to a temperature of $21^\circ C$.

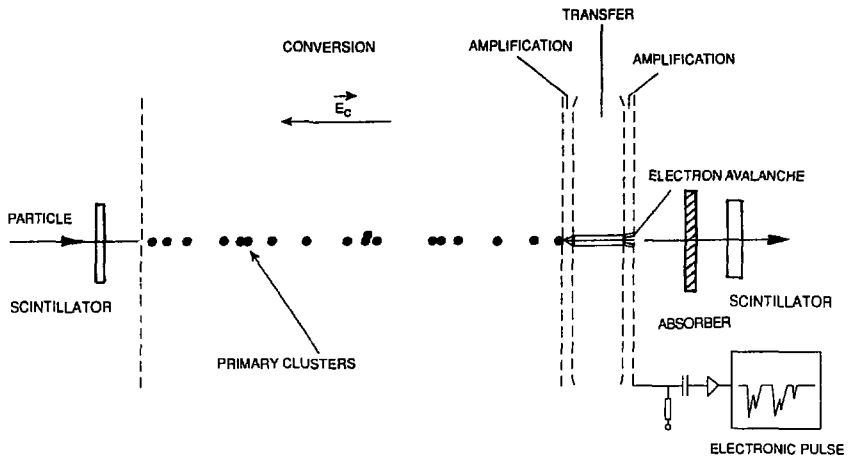


Fig 1.

10 Torr DME

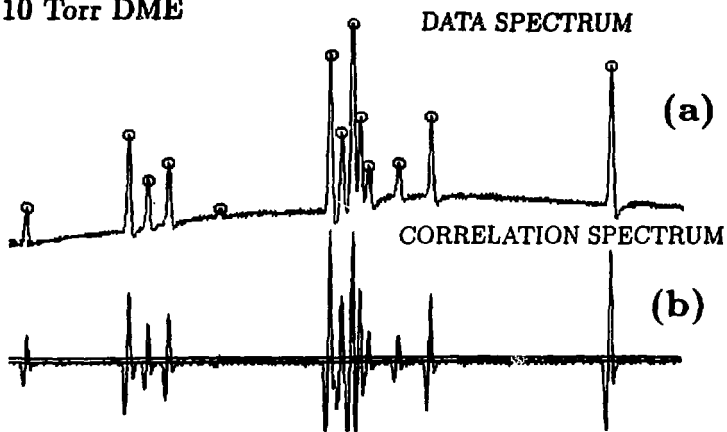


Fig 2.

Efficiency (ϵ) for e^- detection (%)	$P_{N_p=0}$ (observed)	$\frac{SPI_{measured}}{SPI_{true}}$	Error (%)
100	0.2208	1.00	0
99	0.2235	0.992	-0.8
98	0.2263	0.983	-1.7
97	0.2291	0.975	-2.5
96	0.2320	0.967	-3.3
95	0.2349	0.959	-4.1
94	0.2378	0.951	-4.9
92	0.2459	0.934	-6.6
90	0.2500	0.918	-8.2
85	0.2662	0.876	-12.4

Table 1

Gas	PRESENT WORK				RIEKF [14]
	Direct counting		0-counting		0-counting
	SPI ($cm \cdot Torr$) ⁻¹	Accuracy	SPI ($cm \cdot Torr$) ⁻¹	Accuracy	SPI ($cm \cdot Torr$) ⁻¹ Accuracy: see caption
<i>i</i> -C ₄ H ₁₀	0.122	±10%	0.120	-3 + 5%	0.109
C ₃ H ₈	0.097	±10%	0.095	-3 + 5%	0.088
C ₂ H ₆	0.067	±10%	0.065	-3 + 5%	0.053
CH ₄	0.046	see text	0.034	-3 + 5%	0.032
DME	0.082	±10%	0.082	-3 + 5%	0.081
TEA	0.19	±10%	0.195	-4 + 6%	—
TMAE	—	—	0.370	-3 + 5%	—
Argon	0.025-0.050	see text	0.029	-12 + 15%	0.030

Table 2

Pressure (Torr)	Detector Temperature (° C)	SPI ($cm \cdot Torr$) ⁻¹	Statistical accuracy (%)
8.86	66.5	0.122	± 2%
8.55	25.5	0.118	± 3%
8.45	24.0	0.121	± 3.3%
5.08	25.0	0.119	± 2.6%

Table 3

Gas pressure (Torr)	w ($cm/\mu s$)	SPI ($cm \cdot Torr$) ⁻¹
8.0	2.79	0.0965
10.0	2.56	0.0975
12.0	1.98	0.0968

Table 4

Pressure (Torr)	SPI ($cm \cdot Torr$) ⁻¹	Statistical accuracy (%)
1.48	0.369	± 1.9%
2.21	0.363	± 2%
2.32	0.375	± 2.3%

Table 5